Molecular Microbiology (2011) 79(5), 1204–1219 ■
doi:10.1111/j.1365-2958.2010.07512.x
First published online 5 January 2011

Giardia lamblia low-density lipoprotein receptor-related protein is involved in selective lipoprotein endocytosis and parasite replication

Maria R. Rivero,[1] Silvana L. Miras,[1] Rodrigo Quiroga,[2] Andrea S. Rópolo[1] and Maria C. Touz[1]*

[1]*Instituto de Investigación Médica Mercedes y Martín Ferreyra, INIMEC – CONICET, Friuli 2434, Córdoba, Argentina.*

[2]*Centro de Investigaciones en Química Biológica de Córdoba, CIQUIBIC (UNC-CONICET), Departamento de Química Biológica, Facultad de Ciencias Químicas, Universidad Nacional de Córdoba, Ciudad Universitaria, X5000HUA Córdoba, Argentina.*

Summary

As *Giardia lamblia* is unable to synthesize cholesterol *de novo*, this steroid might be obtained from the host's intestinal milieu by endocytosis of lipoproteins. In this work, we identified a putative *Giardia lamblia* low-density lipoprotein receptor-related proteins (GILRP), a type I membrane protein, which shares the substrate N-terminal binding domain and a FXNPXY-type endocytic motif with human LRPs. Expression of tagged GILRP showed that it was localized predominantly in the endoplasmic reticulum, lysosomal-like peripheral vacuoles and plasma membrane. However, the FXNPXY-deleted GILRP was retained at the plasma membrane suggesting that it is abnormally transported and processed. The low-density lipoprotein and chylomicrons interacted with GILRP, with this interaction being necessary for lipoprotein internalization and cell proliferation. Finally, we show that GILRP binds directly to the medium subunit of *Giardia* adaptor protein 2, indicating that receptor-mediated internalization occurs through an adaptin mechanism.

Introduction

The low-density lipoprotein receptor-related protein (LRP) is a large, highly conserved receptor that binds numerous types of ligands, raises several different signal transduction pathways, and is implicated in a variety of diseases including Alzheimer's disease, cancer and HIV (reviewed in Herz and Strickland, 2001). LRP is a member of the low-density lipoprotein receptor (LDLR) family, which also includes the apoE receptor 2 (ApoER2), the very-low-density lipoprotein receptor (VLDLR), multiple epidermal growth factor (EGF) repeat-containing protein (MEGF7), megalin, LDL-related protein-1 (LRP1) and LDL-related protein-1b (LRP1b) (Krieger and Herz, 1994; Willnow *et al.*, 1999; Rebeck *et al.*, 2006). The most characteristic structural components of these receptors are five common structural units: (i) cysteine-rich ligand-binding repeats, which form ligand-binding domains, (ii) EGF receptor-like cysteine-rich repeats, (iii) YWTD domains, (iv) a single membrane-spanning segment and (v) a cytoplasmic tail that contains between one and three FXNPXY-like motifs (Fig. 1) (Jeon *et al.*, 2001; Li *et al.*, 2001; Takeda *et al.*, 2003). Through its binding domains, LRP interacts and mediates the internalization of a diverse group of molecules, ranging from lipoproteins (including apolipoprotein E, chylomicrons, very-low-density lipoprotein and lipoprotein lipase), proteinases and proteinase inhibitor complexes to unrelated molecules (such as lactoferrin and thrombospondin) (reviewed in Herz and Strickland, 2001). Because LRP is a protein which travels along the secretory route, it displays reticular endoplasmic reticulum (ER) and perinuclear Golgi-like staining, in addition to being present at the plasma membrane and within early endosomes (Waldron *et al.*, 2008). During its journey to the cell surface, LRP undergoes sequential cleavage events due to different proteinases (reviewed in Rebeck *et al.*, 2006). LRP is synthesized as a 600 kDa transmembrane glycoprotein, which later becomes cleaved by furin in the *trans*-Golgi network, thus producing a 515 kDa α-subunit and an 85 kDa β-subunit (Herz *et al.*, 1990). These two subunits remain non-covalently associated during transport to the cell surface as well as during internalization and recycling from early endosomes to the plasma membrane (Ward *et al.*, 1989; Herz *et al.*, 1990). The cytoplasmic tail contains FXNPXY-like motifs that serve as docking sites for the endocytosis machinery and for cytoplasmic

Accepted 9 December, 2010. *For correspondence. E-mail ctouz@immf.uncor.edu; Tel. (+54) 351 468 1465; Fax (+54) 351 469 5163.

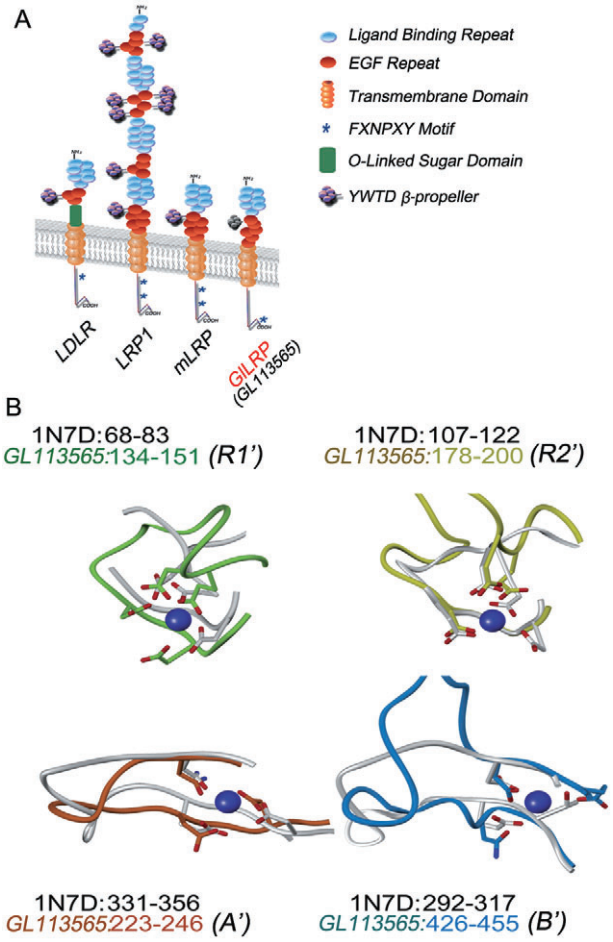

Fig. 1. GILRP as an LDL receptor family member.
A. LDLR and LRP1 represent two of the receptor family members in mammalian cells. LRP minireceptor (mLRP) is used in mammalian cells to examine the ligand-binding properties of LRP (Obermoeller-McCormick *et al*., 2001) and the structure shows a strong similarity with GL113565 putative GILRP (GILRP in red). Each member contains a single transmembrane domain, at least one ligand-binding domain, EGF repeat, YWTD β-propeller and cytoplasmic FXNPXY-like motif. YWTD β-propeller-like domain in GILRP is depicted in grey.
B. Structures of four putative calcium-binding pockets from GL113565. Homology-modelled structures are compared with model structures (partial reproductions of human LRP pdb 1N7D). Labels for each structure indicate the amino acid ranges modelled. The top models correspond to the R1′ and R2′ ligand-binding domain calcium pockets while the lower models correspond to the A′ and B′ EGF precursor homology domain calcium pockets.

adaptors. However, the mechanisms involved in the endocytosis of the members of the LDL receptor family are not completely understood. Moreover, the initial endocytosis rates of individual LDLR family members are significantly different, suggesting that the endocytic functions among these members are distinct.

Although host cell cholesterol has been implicated in the survival and replication of many pathogens, the lipid uptake in protozoa parasites has not been widely characterized. The divergent eukaryote *Giardia lamblia* is unable to synthesize cholesterol *de novo*, although this steroid might be obtained by trophozoites from the intestinal milieu (Lujan *et al*., 1996a; Adam, 2001). It has been shown that a portion of the lipid uptake may be associated with endocytosis of lipoproteins by the trophozoite *in vitro* (Lujan *et al*., 1996a; Rivero *et al*., 2010). For more than a decade, different groups have searched for the LDLR in *Giardia* without success. However, it was suggested that a protein capable of binding LDL may exist in this parasite (Lujan *et al*., 1996a; Rivero *et al*., 2010). It was also proposed that cholesterol is captured from LDL by the C_k-like receptor, thus regulating encystation (Kaul and Kaur, 2001). Nevertheless, no classical lipoprotein receptor has been identified until now. Searching the *Giardia* genome database (GiardiaDB) for genes that codified for homologous LDLR yielded negative results. However, when looking specifically for the characteristic structural motifs of this family receptor, we found a type I membrane protein that contains two cysteine-rich ligand binding repeats and two EGF precursor domains, is homologous to LRP1 and LRP1b, and has one FXNPXY-like internalization signal (FNSPTY) within its cytoplasmic tail. In this study, we examined whether a putative GILRP was responsible for the uptake of cholesterol via its interaction with lipoproteins. Our data indicate that evolutionarily conserved motifs in GILRP mediate direct interactions between GILRP/lipoproteins and the GILRP/μ2-adaptin subunit of the clathrin-adaptor protein 2 (AP2) in this parasite.

Results

The GL113565 Giardia *protein possesses structurally conserved LDLR domains*

Members of the LDLR family are composed of modular domains which include cysteine-rich complement-type repeats, EGF repeats, YWTD β-propeller domains, a transmembrane domain and a cytoplasmic domain. The extracellular complement-type repeats are found in clusters and are implicated not only in ligand binding but also in calcium binding. In a GiardiaDB survey, we identified two proteins containing calcium-binding EGF-like domains (GL113565 and GL94510), similar to the ones found in the LRP of different cells. These *Giardia* proteins were predicted type I membrane proteins homologous to human LRP1 and LRP1b, and possessed a signal peptide, a 20 aa transmembrane domain and a cytoplasmic tail. Interestingly, GL113565 but not GL94510 contained an FXNPXY-like motif (FNSPTY) within its cytoplasmic tail, consistent with the presence of one or more copies of the FXNPXY-like motif in the cytoplasmic domain of the LDLR family members (Fig. 1A). Similar to human LDLR and LRPs, the

extracellular domain of GL113565 was composed of EGF precursor homology domains and several ligand-binding domains (Fig. S1 and Fig. 1B). Models of GL113565 extracellular domains were obtained by homology modelling using Modeller (Sali *et al.*, 1995), based on the crystal structure of the human LDLR (LDLR) extracellular domain (PDB code 1N7D) at 3.7 Å (Rudenko *et al.*, 2002). The model that was generated was structurally similar to the template and contained two well-conserved ligand-binding domains, R1′ (residues 134–151) and R2′ (178–200), and two EGF precursor homology domains, A′ (residues 223–246) and B′ (426–455) (Fig. 1B). Despite the close resemblance between the extracellular domain structures of GL113565 and LDLR, there was little overall sequence similarity suggesting that GL113565 might possess additional non-conserved ligand-binding domains. The region of GL113565 which lies between the EGF precursor homology domain and the transmembrane domain was enriched in beta-sheets according to secondary structure prediction (beta-propeller-like domain) (Fig. S2). However, we were unable to produce a satisfactory model of this region when using the LDLR beta-propeller domain as a template. Because the *Giardia* protein GL113565 fulfils all the structural requirements for an LRP, we further tested whether this protein also functioned as an LRP. For ease of understanding, GL113565 will now be referred to GlLRP.

GlLRP is highly processed

We generated three constructs expressing GlLRP (LRP–HA, HA–LRP and LRP$_{\text{-FXNPXY}}$–HA) (Fig. 2A). To facilitate immunodetection, an HA epitope was included at the C-terminus of GlLRP generating the version LRP–HA. To obtain the N-terminus-tagged GlLRP, the HA epitope was inserted immediately after GlLRP's signal peptide, producing the HA–LRP fusion protein. The LRP$_{\text{-FXNPXY}}$–HA truncated version of GlLRP was generated by deletion of the FXNPXY-like motif and addition of the HA epitope at the C-terminus. *Giardia* trophozoites with stable expression of these receptors were initially identified via immunofluorescence with anti-HA monoclonal antibody (mAb), further purified by subcloning and confirmed by immunoblotting. Thus, we used selected *lrp–ha, ha–lrp* and *lrp$_{\text{-FXNPXY}}$–ha* strains expressing the LRP–HA, HA–LRP and LRP$_{\text{-FXNPXY}}$–HA proteins, respectively, to investigate GlLRP. Consequently, the HA fusion proteins allowed us to independently observe the C- and the N-termini of GlLRP (LRP–HA and HA–LRP respectively) by immunoblot analysis of stably transfected cells. The molecular weight of the most significant bands detected were approximately 116 kDa, 64 kDa and 52 kDa (Fig. 2B, -inh). The ~116 kDa band observed for both LRP–HA and HA–LRP might represent the endoplasmic

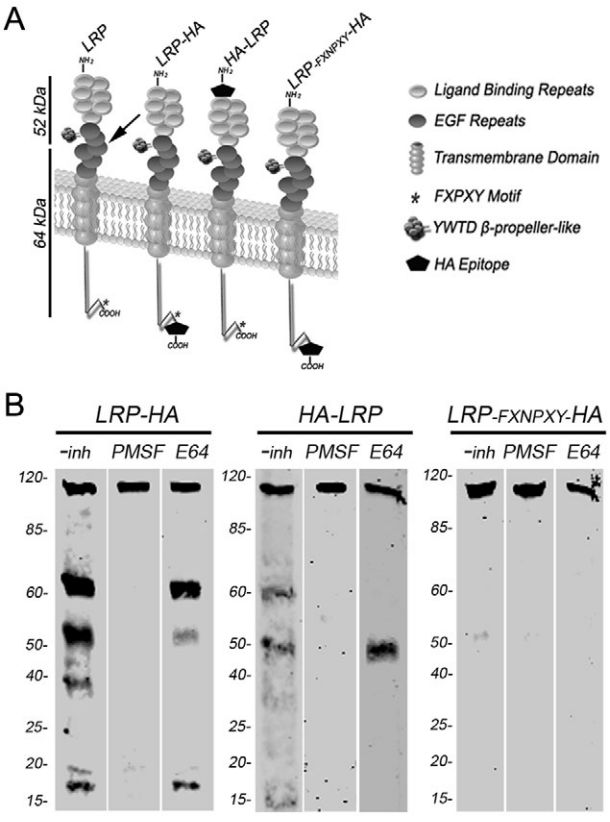

Fig. 2. Processing of GlLRP in stably transfected trophozoites. A. Schematic representation of HA-tagged LRPs is depicted in comparison with the full-length endogenous GlLRP. The putative RPRNT site of furin cleavage (residues 491–495) is represented by an arrow. The presumed subunits (52 and 64 kDa) generated upon furin cleavage are indicated. The HA epitope is shown in black. B. LRP–HA, HA–LRP and LRP$_{\text{-FXNPXY}}$–HA are detected by immunoblotting using anti-HA mAb in 10^3 *lrp–ha, ha–lrp* and *lrp$_{\text{-FXNPXY}}$–ha* trophozoites respectively. Note the significant processing of LRP–HA and HA–LRP in comparison with LRP$_{\text{-FXNPXY}}$–HA (-inh). Addition of the furin-like inhibitor PMSF completely prevented the processing of LRP–HA and HA–LRP (PMSF). Treatment with the cysteine protease inhibitor E64 reduced LRP–HA and HA–LRP cleavage although the main bands of 52 and 64 kDa are still observed (E64). No inhibitory effect is observed for LRP$_{\text{-FXNPXY}}$–HA after treatment (PMSF and E64). Relative molecular weights of protein standards (kDa) are indicated on the left.

reticulum precursor while the other bands might represent the mature subunits of GlLRP after protease processing as was shown for the LRP family (Duckert *et al.*, 2004). To assess whether a furin-like protease is involved in the maturation of GlLRP, the transgenic cells were grown in medium containing the furin inhibitor PMSF (Ashworth *et al.*, 1999a,b) before analysis by immunoblotting. The results showed that the proteolytic process of GlLRP was completely prevented by 170 μg ml^{-1} PMSF, indicated by the presence of only the 116 kDa form in both cells (Fig. 2B, PMSF). Interestingly, addition of the cysteine protease inhibitor E64 significantly reduced LRP process-

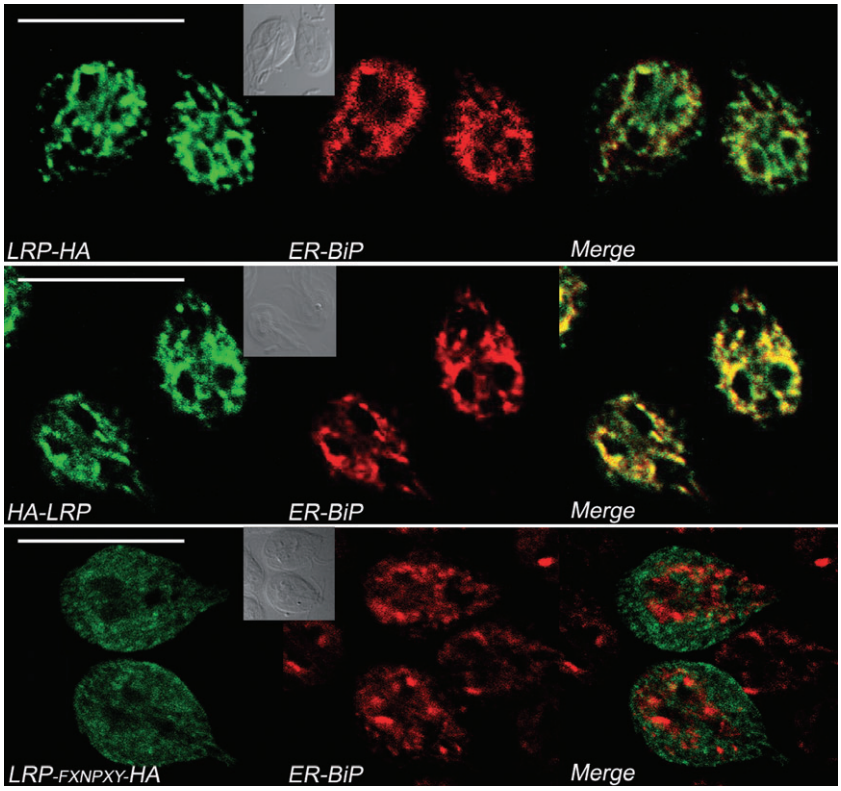

Fig. 3. ER retention of GlLRP is avoided by deletion of the FXNPXY-like motif. Direct IFA and confocal microscopy shows that both LRP–HA and HA–LRP (green) strongly colocalize (merge) with the ER protein BiP (red). LRP$_{\text{-FXNPXY}}$–HA (green) is not present in the ER, showing mostly a cytoplasmic distribution. Inserts show the differential interference contrast (DIC) microscopy. All images were acquired and processed identically. Bars, 10 μm.

ing, although the main bands were still present after treatment (Fig. 2B, E64). The ~ 64 kDa band, expected to contain the transmembrane domain and cytoplasmic tail, was observed for LRP–HA while the ~ 52 kDa band, possibly representing the extracellular subunit of GlLRP, was observed only for HA–LRP (Fig. 2A and B). Addition of the serine protease inhibitors TLCK and TPCK did not have any effect on GlLRP processing (not shown). These results suggest that GlLRP goes through a combination of furin-like and cysteine protease proteolytic events. Moreover, the cleavage performed by a furin-like protease seemed to be necessary for the further action of cysteine proteases likely in the PVs. When LRP$_{\text{-FXNPXY}}$–HA was analysed by immunoblotting before and after the treatment with the proteases inhibitors, only the 116 kDa form was observed. It is thus possible that the deletion of the FXNPXY-like motif in LRP$_{\text{-FXNPXY}}$–HA impaired the proteolytic maturation of GlLRP and the degradation following internalization, as was previously suggested for LRP1 (Reekmans *et al*., 2010).

Deletion of the FXNPXY-like motif impaired ER localization of GlLRP

Previous studies have shown that LRP1 and LRP1b are mainly retained at the ER, a required step in assuring the correct folding and maturation of these receptors (Reekmans *et al*., 2010). To investigate whether this was also the case for GlLRP, we performed colocalization studies and compared the subcellular localization of LRP–HA, HA–LRP and LRP$_{\text{-FXNPXY}}$–HA with the distribution of the ER protein BiP by direct immunofluorescence labelling and confocal laser scanning microscopy (Fig. 3). Both LRP–HA and HA–LRP were found to display a reticular pattern, colocalizing with BiP. However, when LRP$_{\text{-FXNPXY}}$–HA was analysed, this variant receptor was distributed in the cytoplasm and did not colocalize with BiP (Fig. 3). This suggests that the FXNPXY-like motif is essential for early steps in the GlLRP biosynthesis.

GlLRP localizes on the cell surface

After passage through the secretory pathway, the LRPs remain on the cell surface where they bind different substrates via their extracellular portion. To explore cell surface localization of GlLRP, *lrp–ha, ha–lrp* and *lrp$_{\text{-FXNPXY}}$–ha* cells were tested by IFA on fixed, non-permeabilized cells, with HA–LRP being the only GlLRP version detected (not shown). Co-immunostaining of fixed, non-permeabilized *ha–lrp* cells with anti-HA mAb and anti-surface protein 9B10 mAb showed colocalization of both proteins at the plasma membrane (Fig. 4). However, IFA of *lrp–ha* and *lrp$_{\text{-FXNPXY}}$–ha* cells selectively permeabilized with saponin showed colocalization of LRP–HA and $_{\text{FXNPXY}}$–HA with VSP9B10 (Fig. 4). These experiments also confirmed the predicted topology of the

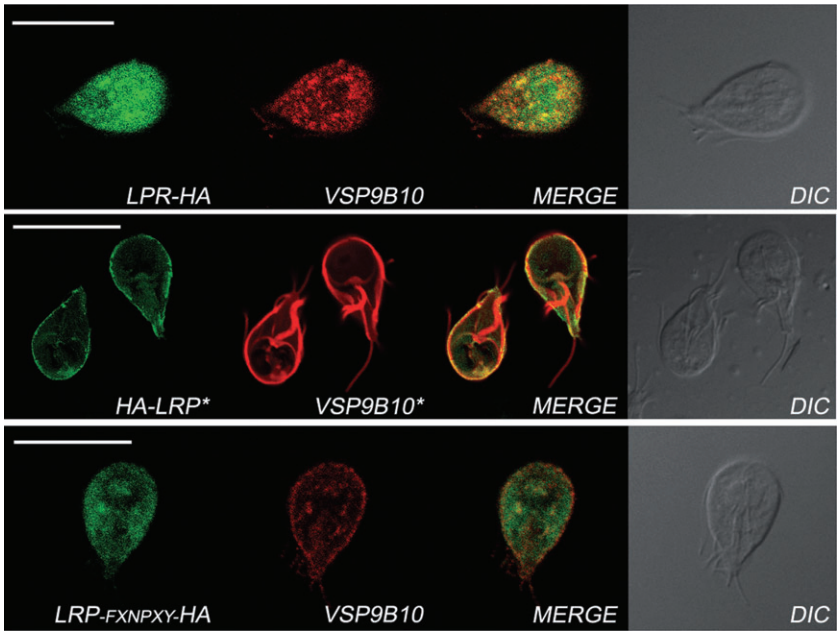

Fig. 4. Surface localization of GlLRP. Direct IFA and fluorescence microscopy show that LRP–HA, HA–LRP and LRP$_{\text{-FXNPXY}}$–HA (green) colocalize with the variant-specific surface protein VSP9B10 (red) at the plasma membrane. *lrp–ha* and *lrp*$_{\text{-FXNPXY}}$*–ha* trophozoites were treated with 0.05% saponin after fixation to selectively permeabilize the plasma membrane. *ha–lrp* cells were fixed and stained without permeabilization (*). Differential interference contrast (DIC) microscopy is shown on the right. All images were acquired and processed identically. Bars, 10 μm.

receptor with the N-terminus exposed to the extracellular space and the C-terminus located inside the cell.

Because total internal reflection fluorescence microscopy (TIRFM) is suitable for imaging transmembrane receptors located at the plasma membrane, we used this technique to corroborate cell surface localization of GlLRP (Fig. 5A) (Axelrod, 1989). For this, *Giardia* cells expressing HA-tagged LRPs were fixed, incubated with saponin (except for *ha–lrp*), labelled with FITC anti-HA mAb and, after a second fixation and attachment, imaged using TIRFM optics. In agreement with previous studies examining LRP1 (Herz *et al*., 1988; Zemskov *et al*., 2007), we observed that the signal was restricted to fluorescent structures close to the plasma membrane of LRP–HA, HA–LRP and LRP$_{\text{-FXNPXY}}$–HA in *lrp–ha, ha–lrp* and *lrp*$_{\text{-FXNPXY}}$*–ha* trophozoites respectively (Fig. 5B). Because the region visualized using TIRFM is at least a few hundred nanometres wide, the cytoplasmic zone immediately beneath the plasma membrane is necessarily visualized in addition to the plasma membrane. To analyse whether the signal obtained allowed the selective visualization of GlLRP in surface regions, the anti-VSP9B10 mAb and the PV-marker LysoSensor (Touz *et al*., 2002a) were used for positive and negative controls respectively. We observed that this methodology was able to detect the surface signal from VSP9B10 but not from the PV-fluorescent marker LysoSensor in saponin-permeabilized cells (Fig. 5B).

GlLRP is associated with lipoproteins

Mammalian LRP is larger than but structurally similar to other members of the LDLR protein family. Whereas LDLR acts in lipoprotein metabolism binding LDL via the single protein apolipoprotein B-100 (apoB-100), the LRP appears to be important for the clearance of apo-B48-containing lipoproteins such as chylomicrons. Recently, we showed that LDL is internalized and delivered to the PVs by adaptin-mediated endocytosis in *Giardia*, a process that requires specific binding of LDL to a receptor (Rivero *et al*., 2010). To analyse whether GlLRP functions as an LDL receptor in this parasite, we performed an assay of fluorescent Bodipy-LDL uptake in *lrp–ha*, followed by immunofluorescence and confocal microscopy analysing different optical section planes from the surface (Fig. 6, a–e). The results showed that Bodipy-LDL partially colocalized with LRP–HA in a cluster-like pattern on transgenic trophozoites.

To determine the *in vivo* interaction between LRP and LDL, *lrp–ha, ha–lrp* and *lrp*$_{\text{-FXNPXY}}$*–ha* trophozoites were grown in lipoprotein-deficient medium followed by incubation in labelling medium containing LDL for up to 2 h. After removing the unbound LDL by washing, LDL was immunoprecipitated with an antibody against ApoB and the immunoprecipitate was subsequently separated by SDS-PAGE and detected by immunoblot using a directly labelled anti-HA mAb (revealing the HA-tagged LRPs). The immunoprecipitation assays (IPP) showed that the tagged LRPs were able to bind LDL because they were all co-immunoprecipitated with the anti-ApoB mAb, suggesting a functional interaction (Fig. 7A). Apo-B48, a truncated apoB-containing the N-terminal portion of apo-B100, is required for the assembly of chylomicrons in the intestine. Our recent studies showed that LDL and chylomicrons, but not ApoA-containing high-density lipoprotein (HDL), impaired LDL endocytosis (Rivero *et al*., 2010). To deter-

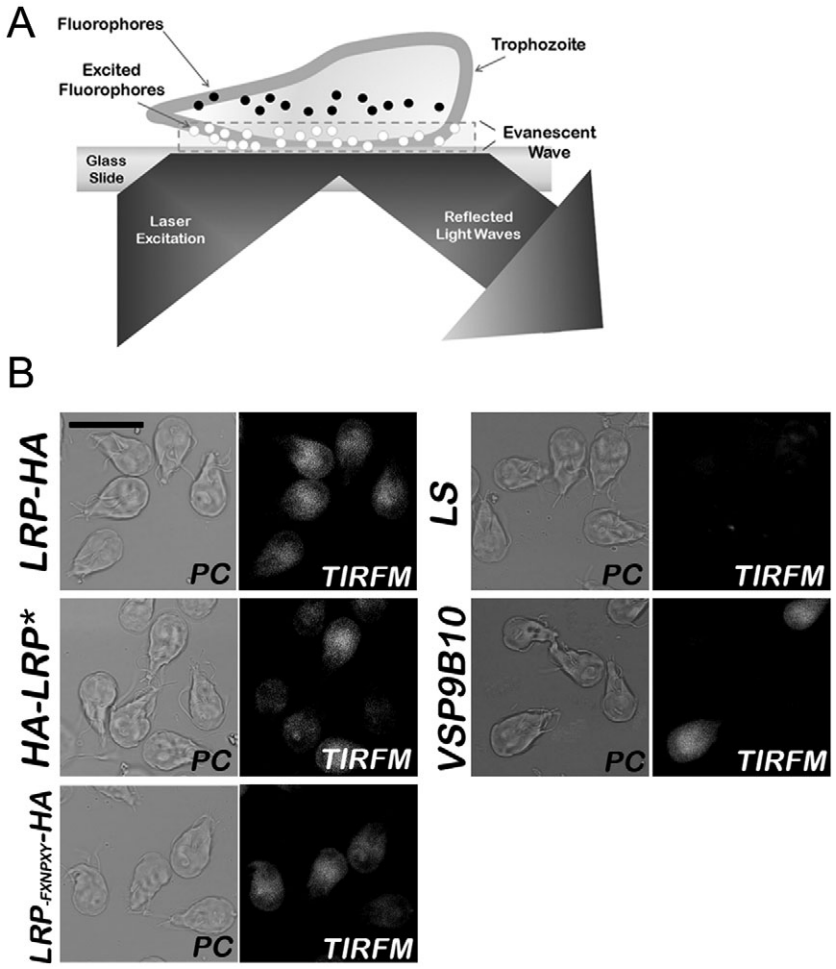

Fig. 5. Plasma membrane localization of GlLRP by TIRFM.
A. Schematic illustration of a *Giardia* trophozoite attached to the glass slide by its dorsal side during TIRFM. When the incidence angle of laser excitation entirely reflects the illuminating beam back, a specific fluorescent excitation (evanescent wave) is induced in a very thin optical section from the glass surface (≤ 100 nm in depth). This evanescent wave is an electromagnetic field which decays exponentially; thus, only the fluorophores nearest the glass surface (e.g. plasma membrane proteins) are selectively excited (O) (adapted from Axelrod, 2003).
B. TIRFM show LRP–HA, HA–LRP, LRP$_{\text{-FXNPXY}}$–HA and VSP9B10 at the plasma membrane. The PV-marker LysoSensor (LS) does not present fluorescence at the surface. The trophozoites were treated with 0.05% saponin after fixation to selectively permeabilize the plasma membrane except for *ha–lrp* cells that were fixed and stained without permeabilization (*). Phase-contrast images are depicted on the left panels (PC). All images were acquired and processed identically. Bars, 10 μm.

mine whether GlLRP might also be a receptor for chylomicrons, we repeated the immunoprecipitation utilizing the anti-ApoB mAb (that recognizes both ApoB100 and ApoB48 apoproteins) now challenging the transgenic and wild-type trophozoites with purified chylomicrons. We observed that the tagged LRPs co-precipitated with ApoB suggesting that GlLRP is involved in the uptake of cholesterol from chylomicrons in this parasite (Fig. 7B). IPP control utilizing LRP–HA strain extracts in the absence of added LDL or chylomicrons showed no detection of the HA-tagged LRP (Fig. 7A and B, control). There was also no indication of tagged LRP when wild-type cells or transgenic cells were immunoprecipitated with anti-ApoB or a non-related anti-V5 mAb respectively (not shown). When the trophozoites were grown in medium containing the protease inhibitor PMSF before lipoprotein challenge, only the 116 kDa band was observed after ApoB immunoprecipitation confirming that the LRP precursor was able to bind LDL and chylomicrons (Fig. 7C). These results represent the first demonstration of the interaction between lipoproteins and a membrane receptor in this parasite.

GlLRP down- and upregulation controls LDL internalization

We sought to establish a functional connection between GlLRP and LDL endocytosis by reducing GlLRP expression via an antisense RNA approach (Fig. S3A). After transfection and stable selection of trophozoites deficient in GlLRP (*lrp:as*), the depletion of GlLRP expression by antisense production was determined by semi-quantitative RT-PCR. Quantification of the corresponding mRNA showed that the amount of *Giardia lrp* decreased by 83 ± 5% ($n = 5$) in trophozoites expressing the antisense. This depletion, however, had no effect on the steady-state levels of the constitutively expressed glutamate dehydrogenase enzyme mRNA (*gdh*) (Fig. S3B). To study whether LDL was indeed internalized by GlLRP binding, we compared the endocytic uptake and PV delivery of Bodipy-LDL in wild-type, *lrp:as* (GlLRP depleted), *lrp–ha* (GlLRP overexpressed) and *lrp*$_{\text{-FXNPXY}}$*–ha* trophozoites. A significant reduction of LDL internalization was observed when comparing wild-type (*wt*) and *lrp:as* trophozoites from up to 2 h (Fig. 8A). Conversely, an increase in the LDL internaliza-

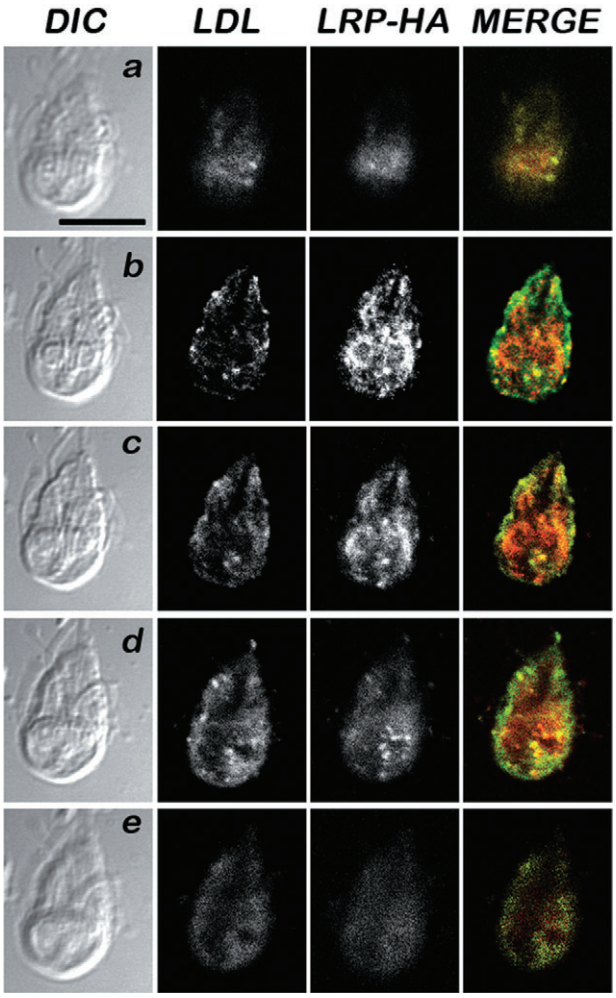

Fig. 6. LDL and GlLRP colocalize in patches. Direct IFA and confocal laser scanning microscopy of *lrp–ha* cells using anti-HA mAb (LRP–HA in red) and Bodipy-LDL (green) show partial colocalization (merge in yellow) at different optical section plains from the surface. From the dorsal to the ventral plane: (a) 0.0 μm, (b) 1.2 μm, (c) 2.4 μm, (d) 3.2 μm and (e) 5.2 μm. Differential interference contrast (DIC) microscopy images of each section are depicted on the left. All images were acquired and processed identically. Bars, 10 μm.

tion over time was detected for *lrp–ha* cells compared with wild type (Fig. 8A). When *lrp*$_{\text{-FXNPXY}}$*–ha* trophozoites were tested, the internalization of Bodipy-LDL was highly delayed showing LDL label in the PVs later than 2 h (Fig. 8A). It is possible that this effect has been a result of the combination of LDL binding to LRP$_{\text{-FXNPXY}}$–HA, which may be unable to internalize LDL, and to the native LRP. Follow-up of LDL internalization in wild-type, *lrp:as*, *lrp–ha* and *lrp*$_{\text{-FXNPXY}}$*–ha* trophozoites for 24 h did not significantly change the observed pattern. Quantitative data from three different uptake experiments are shown in Fig. 8B. Finally, the controls utilizing the fluid-phase marker FITC-dextran or the PV-marker LysoTracker (Touz *et al*., 2003; Rivero *et al*., 2010) did not display differences in the fluid-phase uptake between these cells (Fig. 8C). Overall, the uptake results clearly support our hypothesis that GlLRP is involved in LDL endocytosis in this parasite.

Reduction of GlLRP expression impairs Giardia *growth*

Some studies have suggested that the acquisition of cholesterol via LDL and chylomicrons is necessary to support *Giardia* growth (Lujan *et al*., 1996a; Rivero *et al*., 2010). Thus, it is possible that GlLRP is also required for trophozoite replication. To analyse *Giardia* growth in the absence of GlLRP, time-course curves were performed in *wt* and *lrp:as* cells without the addition of puromycin. Similar to the effect of LDL depletion (Rivero *et al*., 2010), a significant effect of *lrp:as* cells on the growth curve was observed at 24 h post culturing with the maximum effect being achieved at 48 h (Fig. 9). At this time point no cell deterioration was observed. Trophozoites transfected with an empty vector or an unrelated antisense RNA were unable to produce growth inhibition demonstrating that the effect observed might be specifically attributed to GlLRP depletion (Fig. 9).

GlLRP might be endocytosed by Giardia *adaptor protein 2*

The results presented strongly indicate that the binding and endocytosis of LDL depend on GlLRP. In addition, we have previously shown that LDL endocytosis was blocked by downregulation of the medium subunit (μ2) of the heterotetrameric clathrin-adaptor protein AP2 (Rivero *et al*., 2010). Taken together, these results suggest that AP2 might be involved in the binding and internalization of GlLRP in this parasite. To investigate whether GlLRP and μ2 directly interact, we used a yeast two-hybrid assay, in which full-length GlLRP or LRP$_{\text{-FXNPXY}}$ was expressed in frame with the activation domain encoded by **p**GADT7 (AD), while μ2 was expressed in frame with the DNA-binding domain encoded by **p**GBKT7 (BD). The expression of approximately equal levels of protein from all constructs was confirmed by immunoblots of yeast protein extracts following transformation (data not shown). The interaction of GlLRP with μ2 was observed by the growth of yeast cells on medium lacking leucine, tryptophan and histidine (TDO), which selects for colonies expressing interacting proteins (Fig. 10A). By using a high-stringency medium that also lacked adenine (QDO), we demonstrated that this interaction was both strong and direct (Fig. 10A). Importantly, the LRP$_{\text{-FXNPXY}}$–AD construct, which lacks the FXNPXY-like motif of GlLRP, exhibited no growth in combination with μ2 (Fig. 10A, TDO-QDO). To confirm the μ2–GlLRP interaction, we performed IPP using *lrp–ha* and *lrp*$_{\text{-FXNPXY}}$*–ha* trophozoites and a mAb that specifically recognizes μ2. As shown in

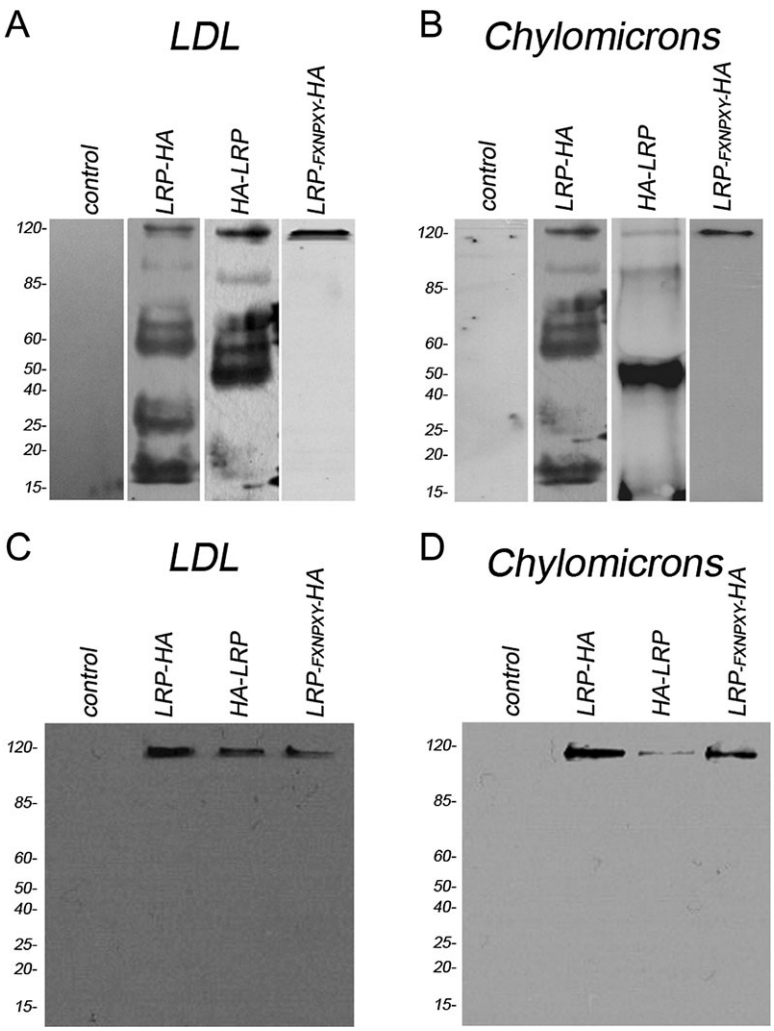

Fig. 7. GlLRP binds lipoproteins.
Immunoblotting after IPP utilizing anti-ApoB mAb.
A. LRP–HA co-immunoprecipitates with ApoB in *lrp–ha, ha–lrp* and *lrp*$_{\text{-FXNPXY}}$*–ha* trophozoites after 2 h of LDL uptake. The control cells without LDL do not show non-specific binding under the same IPP conditions.
B. LRP–HA co-precipitates with ApoB after 2 h of incubation with chylomicrons (2 h). There is no label of LRP–HA when the transgenic cells were treated in the absence of chylomicrons (control).
C. Addition of the protease inhibitor PMSF shows the co-immunoprecipitation of the LDL-ApoB and the putative precursor of GlLRP.
D. Co-immunoprecipitation of chylomicrons-ApoB and GlLRP precursor after addition of PMSF. Controls included the omission of lipoprotein. The immunoblot experiments were performed utilizing alkaline phosphatase-labelled anti-HA mAb.
Relative molecular weights of protein standards are indicated on the left in kDa.

Fig. 10B, LRP–HA co-immunoprecipitated with μ2 (LRP–HA, line 2) while LRP$_{\text{-FXNPXY}}$–HA was unable to precipitate in concert with μ2 (LRP$_{\text{-FXNPXY}}$–HA, line 2), reinforcing the idea that the endocytic motif is crucial for GlLRP-μ2 interaction.

The colocalization of GlLRP and μ2 was analysed by direct immunofluorescence and confocal microscopy utilizing the anti-μ2 mAb in *lrp–ha* trophozoites. Previously, we showed that μ2 localized mainly in the PVs, with some cytoplasmic and plasma membrane localization also observed in growing trophozoites (Rivero *et al.*, 2010). Although most of the LRP–HA labelling was noted in association with the ER, partial colocalization with μ2 was detected in the PVs (Fig. 11A). An analysis of 100 cells confirmed that the colocalization was similar in all cells. Interestingly, in many of these cells, a nuclear localization of LRP–HA was detected, thus implying the participation of this receptor in cell signalling, as has been extensively described for the LRP family (see *Discussion*). Additional studies detecting LRP$_{\text{-FXNPXY}}$–HA and μ2 in *lrp*$_{\text{-FXNPXY}}$*–ha* trophozoites demonstrated that LRP$_{\text{-FXNPXY}}$–HA localized predominantly to the plasma membrane and did not colocalize with μ2 in the PVs (Fig. 11B). In contrast with the results obtained from the expression of LRP–HA, LRP$_{\text{-FXNPXY}}$–HA was neither retained in the ER nor detected in the PVs or nuclei, suggesting an important role of the FXNPXY-like motif in GlLRP transport and subcellular localization.

Discussion

The present study establishes that, in the absence of the LDLR, a protein homologous to LDLR-related protein 1 participates in the endocytosis of ApoB lipoproteins, a process that also depends upon the clathrin-adaptor protein 2 (AP2) in *Giardia*. GlLRP shares structural elements with all members of the LDLR family, with the extracellular segments, which are responsible for the binding and release of their lipoprotein ligands, containing ligand-binding domains and EGF-like cysteine-rich

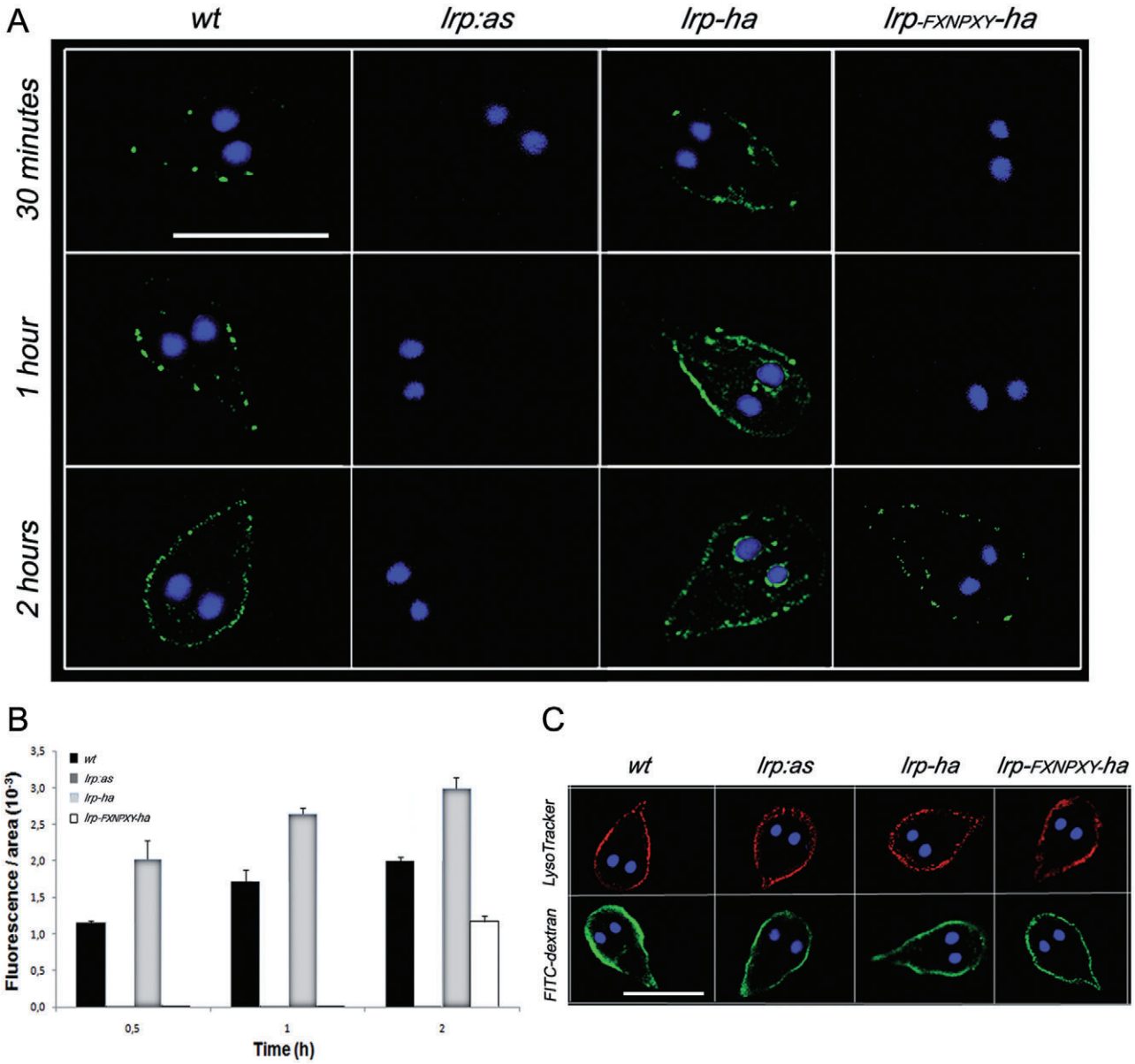

Fig. 8. The endocytosis of LDL depends of the level of GlLRP expression.
A. Immunofluorescence microscopy shows that Bodipy-LDL is endocytosed to the PVs in wild-type trophozoites (*wt*) but not in *lrp:as* trophozoites (up to 2 h). *lrp–ha* cells overexpressing LRP–HA show an increase of LDL internalization over time. *lrp-FXNPXY–ha* trophozoites show a remarkable delay in LDL endocytosis and PV delivery. The most representative effect is shown for each type of cell. Bar, 10 μm. Nuclear DNA was labelled with 4′,6-diamidino-2-phenylindole (DAPI) (blue).
B. Histograms of fluorescent images (fluorescence/area × 10^3) show the relative amount of Bodipy-LDL internalized by parasites in control (*wt*) and transgenic cells (*lrp–ha*, *lrp-FXNPXY–ha* and *lrp:as*). All images were equally processed; the threshold value was determined and is exclusive in each image. The results are presented here as the average (± SD) of 10 determinations.
C. Controls adding LysoTracker Red or FITC-dextran for 30 min show no alteration of fluid-phase endocytosis in all cell types. Bar, 10 μm.

repeats. The YWTD motif, which is proposed to form a β-propeller domain, is not conserved in the GlLRP sequence, thus suggesting that the lipoprotein release at low pH and the recycling of the receptor to the cell surface might be somewhat different in this parasite (Rudenko *et al*., 2002). GlLRP also contains a single membrane-spanning region and a cytoplasmic tail containing an FXNPXY-like motif, which serves to regulate the endocytic and signalling functions of these receptors (Goretzki and Mueller, 1998; Trommsdorff *et al*., 1998; 1999; Misra *et al*., 1999). Given the lack of an LDLR-homologous protein, GlLRP seems to be a reliable candidate for lipoprotein binding and cholesterol uptake by *Giardia* trophozoites.

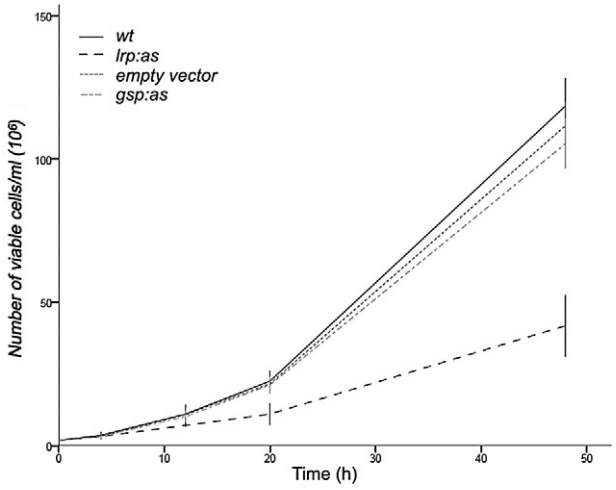

Fig. 9. GlLRP-depleted cells show a decrease in growth. Cell growth curves of *wt* and *lrp:as* trophozoites cultured in presence of LDL for 6, 12, 24, 36 and 48 h. A decrease of cell proliferation capability for *lrp:as* trophozoites is evident. Control cells containing the empty vector or *gsp:as* cells do not show any defect in cell growth comparing with *wt*. Data represent 2 ± SD for $n = 6$ of three independent experiments.

As in the case of other LRP receptors, we found that GlLRP was highly proteolysed. It is possible that GlLRP might be cleaved at a site that matches the consensus sequence recognized by furin, a processing proteinase that frequently serves to activate or modify cell surface receptors and secreted proteins upon exit from the secretory pathway (Steiner, 1998). Notably, furin also cleaves members of the Notch family of cell surface signalling proteins, which, as in LRP, contain multiple EGF repeats in their extracellular domains (Logeat *et al*., 1998). Although there is no experimental evidence, the furin precursor putative serine protease (GL2897) has been found in the *Giardia* genome and its proteolytic activity has been proposed (Touz *et al*., 2002b). In this sense, immunoblotting of different versions of tagged LRP showed that the ER precursor form was partially cleaved mainly into 52 kDa and 64 kDa forms, likely by a furin-like protease. We observed additional shedding of GlLRP and experimentally confirmed that the action of a cysteine protease was involved. Remarkably, deletion of the FXNPXY-like motif impaired GlLRP proteolysis, suggesting a key role of this motif in the process of maturation and degradation. When we analysed the subcellular localization of full-length tagged LRPs, the receptor was observed to be somehow retained at the ER and localized in the PVs and plasma membrane. Conversely, experiments utilizing *lrp-FXNPXY–ha* trophozoites revealed that the majority of the LRP$_{\text{-FXNPXY}}$–HA pool was not retained at the ER before being delivered to the plasma membrane. We also observed that LRP$_{\text{-FXNPXY}}$–HA showed a punctuate cytoplasmic staining, and it is possible that a portion of the immature 'non-cleavable' GlLRP pool did not accumulate in the ER but was rather degraded by the proteasome complex, as was recently described for LRP1 (Reekmans *et al*., 2010). Although LRP$_{\text{-FXNPXY}}$–HA possesses several predicted ubiquitination sites (Tung and Ho, 2008), and the proteosome has been described in *Giardia* (Gallego *et al*., 2007), further studies will be necessary to show whether this mechanism of degradation applies for LRP$_{\text{-FXNPXY}}$–HA. On the other hand, the LRP$_{\text{-FXNPXY}}$–HA that reached the cell surface was unable to be internalized because no distinguishable PV-localization pattern was found. These results argue in favour of a mechanism where GlLRP is shortly retained at the ER for maturation and processing before being delivered to the plasma membrane. Subsequently, GlLRP is internalized via the FXNPXY-like motif to the PVs where it might be degraded or recycled back to the plasma membrane (see below).

Giardia trophozoites do not have the capacity of *de novo* cholesterol synthesis. Instead, they appear to satisfy their lipid requirements by obtaining cholesterol and phosphatidylcholine from the external environment in the duodenum and jejunum *in vivo*, and from the serum component of the modified TYI-S-33 medium *in vitro* (Keister, 1983). In axenic cultures, the cholesterol and phospholipids are supplied by lipoproteins, beta-cyclodextrins and bile salts, with the transfer of lipids to the parasite surface being facilitated by bile salts (Lujan *et al*., 1996a). In a recent report, we showed that *Giardia* trophozoites are able to acquire LDL from the culture medium, with this lipoprotein being critical for parasite growth and survival (Rivero *et al*., 2010). Here, we showed that *in vitro* growth of parasites was significantly inhibited by the reduction of GlLRP expression, providing additional evidence of

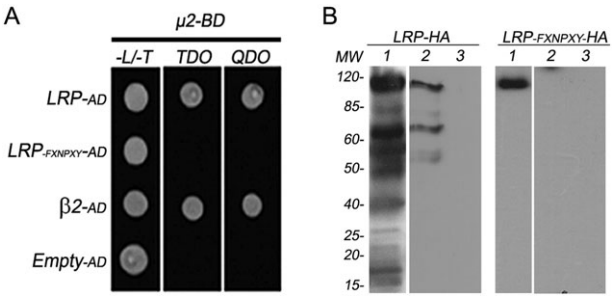

Fig. 10. GlLRP interacts with AP2 via its cytoplasmic endocytic motif.
A. The yeast two-hybrid assay demonstrates that GlLRP but not LRP$_{\text{-FXNPXY}}$ (LRP lacking the endocytic motif) specifically interacts with μ2. β2 and the empty AD vector were used as positive and negative controls respectively.
B. Immunoblotting using HRP-conjugated anti-HA mAb shows LRP–HA and LRP$_{\text{-FXNPXY}}$–HA input before IPP (lines 1). After IPP assays using anti-μ2 mAb, LRP–HA but not LRP$_{\text{-FXNPXY}}$–HA co-precipitates with μ2 (lines 2). Control using non-transfected cells in IPP shows no specific interaction (lines 3). MW standards are shown on the left of the panel in kDa.

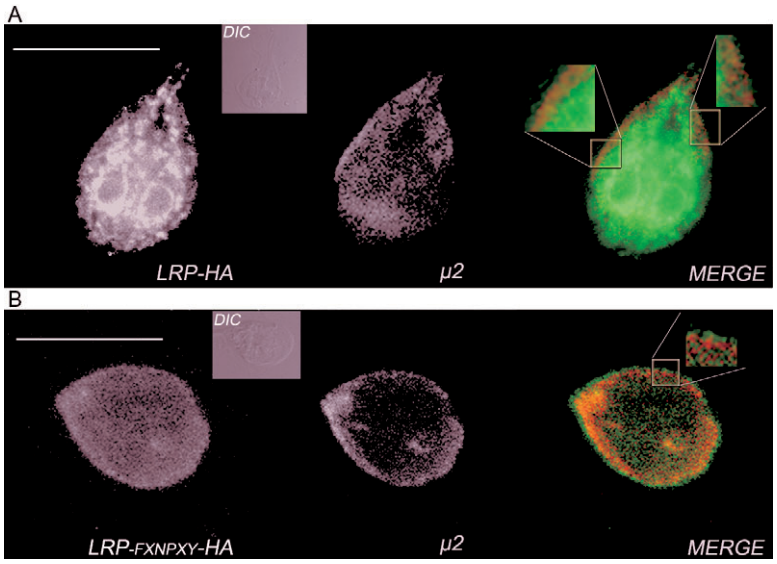

Fig. 11. The subcellular colocalization between GILRP and μ2 depends on the FXNPXY-like motif.
A. Direct IFA and confocal microscopy illustrating that LRP–HA and μ2 partially colocalize in the PVs (colocalization in yellow, magnifications) in *lrp–ha* trophozoites.
B. LRP$_{\text{-FXNPXY}}$–HA is found predominantly at the plasma membrane and does not colocalize with μ2, neither by confocal microscopy examination nor by colocalization analysis (insert). Differential interference contrast microscopy (DIC) is depicted in the inserts.
Bars, 10 μm.

the importance of cholesterol acquisition from serum lipoproteins. We recently showed that the endocytosis of LDL depended on AP2, suggesting that LDL is internalized via a receptor-mediated process (Rivero *et al*., 2010). In the current study, we found that GILRP plays a role in the binding and endocytosis of apoB-containing lipoproteins, probably as a mechanism for cholesterol acquisition. Subcellular localization and protein – protein interaction experiments demonstrate that LDL and GILRP interact via ApoB, with GILRP participating in the binding and uptake of LDL by trophozoites when the expression of the receptor was down- or upregulated. Interestingly, we observed that GILRP behaved like an ApoB receptor in terms of its interactions not only with LDL, but also with chylomicrons. This observation strongly suggests that GILRP plays a fundamental role in the uptake of chylomicrons from the host intestine and is able to recognize ApoB100 apoprotein from LDL in axenic cultures as a way of adapting to a new environment. Our findings are supported by several studies, which show the importance of LRP in the uptake of apo-B48-containing lipoproteins (Veniant *et al*., 1998; Yu *et al*., 2001) as well as in the clearance of lipoproteins in animals that are deficient in the LDL receptor (Willnow and Herz, 1995; Willnow *et al*., 1995; Veniant *et al*., 1998).

One common characteristic of LDLR family members is that they have at least one copy of the FXNPXY-like sequence in their cytoplasmic tail, which serves either as the signal for endocytosis or as a binding element for cellular adaptor proteins involved in signal transduction (Harris-White and Frautschy, 2005). Despite the fact that no LRP-like adaptor proteins that contain a PTB domain, such as ARH or Dab, have been found in the *Giardia* genome, we demonstrated here that GILRP binds to the medium subunit (μ2) of AP2 and that this interaction depends on the FXNPXY-like motif. This finding is in agreement with others that show a failure in GILRP trafficking to the PVs when it lacks the FXNPXY-like motif. Additionally, it has been shown by surface plasmon resonance and photoaffinity labelling that the FXNPXY-like motif binds to μ2 purified from bovine brain-coated vesicles (Boll *et al*., 2002). Interestingly, in spite of the strong interaction found between ARH and LRP1 in an *in vitro* binding assay, the subcellular localization of LRP1 was not affected in the liver of ARH-deficient mice, whereas LDLR was found to be redistributed from intracellular localizations to the cell membrane (Jones *et al*., 2003). This effect underscores the importance of the availability of intracellular adaptor proteins in the determination of the specific cellular function of lipoprotein receptors.

Given the similarities between GILRP and other members of the LRP family, it is also possible that this protein binds several other substrates essential for growth, such as growth factors (Lujan *et al*., 1994) or proteases. Therefore, it is possible that GILRP is multifunctional and is involved in both receptor-mediated endocytosis (which leads to the degradation of the endocytosed material) and in cell signalling. In mammalian cells, proteolytic cleavage of LRP, either within the membrane by gamma-secretase activity or close to the cytoplasmic leaflet, results in the release of this domain into the cytoplasm, where it modulates signalling or is further translocated to other subcellular compartments (Liu *et al*., 2007). Our preliminary results suggest that the degradation of GILRP might in part be due to the action of a gamma-secretase-like complex (M.R. Rivero, unpubl. results). Further investigations are required to reveal if

GILRP provides cross-talk with the signalling pathways to regulate cell growth and differentiation.

In summary, results from the current investigation reveal that a receptor containing the characteristics of an LDLR family member is present in *Giardia* trophozoites. This receptor (GILRP) is implicated in the binding and internalization of lipoproteins showing once more the capacity of this parasite to acquire essential components from different environments. It is, however, important to assess the binding of other ligands as well. An important subject for future studies will be to analyse whether GILRP binding and processing are involved in transcription regulation or activation of components of the signalling pathways during *Giardia* growth and differentiation.

Experimental procedures

Antibodies and other reagents

Anti-HA, HRP-labelled anti-HA, alkaline phosphatase (AP)-labelled anti-HA and FITC-labelled anti-HA mAbs were purchased from Sigma (St. Louis, MO). 9C9 mAb was employed to detect the ER-BiP protein (Lujan *et al*., 1996b). 9B10 mAb was used for the detection of VSP9B10 (Nash *et al*., 2001). Anti-μ2 mAb 2F5 was used for the μ2 subunit of AP2 (Rivero *et al*., 2010). Alexa Fluor 555 was used for the primary antibody label (Zenon Tricolor Mouse IgG1 Labelling Kit, Molecular Probes, Invitrogen, Carlsbad, CA). Bodipy-labelled LDL was purchased from Molecular Probes-Invitrogen. Human chylomicrons were acquired from Athens Research & Technology. The L-*trans*-epoxysuccinyl-leucylamido(4-guanidino)butane (E64) and phenylmethylsulphonyl fluoride (PMSF) were purchased from Sigma (St. Louis, MO). Saponin and Triton X-100 were also purchased from Sigma (St. Louis, MO). LysoSensor™ Green DND-189 and LysoTracker™ Red DND-99 used to label PVs were acquired from Molecular Probes-Invitrogen (Carlsbad, CA). The 20 kDa FITC-dextran was purchased from Sigma (St. Louis, MO).

Sequence alignment. MUSCLE, CLUSTALW2 and manual curation were iteratively used to produce the pairwise alignment between GILRP and human LDLR and LRP1 sequences. Jalview was used to manually curate and produce publication images.

Structure modelling. Modeller 9v7 was used to model putative GILRP calcium-binding pockets using pdb 1N7D as a template (Sali *et al*., 1995). Modelling was performed using symmetry restraints for identical residues between the template and model sequences which interact with calcium atoms. One hundred models were built for each pocket, and the model with the best Modeller objective function values and DOPE scores was depicted (Shen and Sali, 2006).

Giardia *cell lines and vectors*

Trophozoites of the isolate WB, clone 1267 (Nash *et al*., 1988), were cultured in TYI-S-33 medium supplemented with 10% adult bovine serum and 0.5 mg ml^{-1} bovine bile, as previously described (Keister, 1983). These trophozoites were used as hosts for the expression of transgenic genes and as non-transfected controls. The GILRP open reading frame (ORF) was amplified from genomic DNA using the f1 (CATTCCATG GATGCAGTGATCTACGGATTGCTTGTC) and r1 (CAT TGATATCATATGTGGGGCTATTGAAGTCTTCAT) primers and cloned into the plasmid **p**TubHAc-pac (Touz *et al*., 2003) to generate the **p**LRP–HA vector. LRP cDNA lacking the endocytic motif was amplified using the f1 and r1′ (CAT-TGATATCGAAGTCTTCATTGCTTC) primers and cloned into the **p**TubHAc-pac vector to generate the **p**$LRP_{-FXNPXY}$–HA expression plasmid. To generate the N-terminus HA-tagged GILRP, an *lrp* ORF lacking the signal peptide was amplified by using the f2 (CAATACGCGTACCTACATACTGCTATCT CTGTTGTTGA) and r2 (CAATGCGGCCGCCTAATATG TGGGGCTATTGAAGTCTTC) primers and cloned into the pTubH7Pac–HA vector (Kulakova *et al*., 2006). All vectors contained a puromycin cassette under the control of the endogenous non-regulated *gdh* promoter for cell selection. Stable trophozoite transfection was performed as previously described (Yee and Nash, 1995; Singer *et al*., 1998; Elmendorf *et al*., 2001; Touz *et al*., 2004; 2005). Drug-resistant trophozoites were usually apparent by 7–10 days post transfection.

Inhibitor assays

The activities of furin and cysteine proteases were monitored using the specific inhibitors PMSF and E64 respectively. Briefly, 10^4 *lrp–ha*, *ha–lrp* and $lrp_{-FXNPXY}$*–ha* trophozoites were grown in complete medium containing 170 μg ml^{-1} PMSF, 10 μg ml^{-1} E64 or DMSO (for control) for 24 h (Touz *et al*., 2002a). The trophozoites were then chilled, collected by centrifugation and analysed by immunoblotting.

Immunoblot analysis

Immunoblot assays were performed as previously reported (Touz *et al*., 2005). Briefly, 10 μg of total protein was incubated with sample buffer, boiled for 10 min and separated in 10% Bis-Tris gels. Samples were transferred to nitrocellulose membranes, blocked with 5% skim milk and 0.1% Tween-20 in TBS, and then incubated with primary antibody diluted in the same buffer. After washing and incubation with an enzyme-conjugated secondary antibody, proteins were visualized with the SuperSignal West Pico Chemiluminescent Substrate (Pierce) and autoradiography, or by using BCIP/NBT substrate (Bio-Rad). Controls included the omission of the primary antibody, the use of an unrelated antibody or assays using non-transfected cells.

Immunofluorescence assay

Trophozoites were washed with PBSm (1% growth medium in PBS, pH 7.4) and allowed to attach themselves to slides at 37°C. After fixation with 4% formaldehyde, the cells were washed and blocked with PBS containing 10% normal goat serum and 0.1% Triton X-100. The cells were then incubated with specific Abs in PBS containing 3% normal goat serum

and 0.1% Triton X-100, followed by incubation with FITC or Texas red-conjugated goat anti-mouse secondary antibody. For cell surface localization of LRP–HA and LRP-FXNPXY–HA, the transgenic cells were blocked and the plasma membrane selectively permeabilized with 0.05% saponin (Wassler *et al.*, 1987; Delcamp *et al.*, 1998; Newman *et al.*, 2009). For surface staining of HA–LRP, detergent treatment was omitted. For direct double staining, the anti-HA mAb (Sigma, St. Louis, MO) was labelled with Zenon Alexa Fluor 488 and was used to detect HA-tagged LRP (final dilution of anti-HA 1:500), while 9C9, 2F5 and 9B10 mAbs were labelled with Zenon Alexa Fluor 555 (1:200 final dilution), following the manufacturer's suggested protocol (Zenon Tricolor Mouse IgG_1 Labelling Kit, Molecular Probes, Invitrogen Corporation, Carlsbad, CA). Controls included the omission of the primary antibody and the staining of wild-type cells. Finally, preparations were washed and mounted in Vectashield mounting medium. Fluorescence staining was visualized with a motorized FV1000 Olympus confocal microscope (Olympus UK, UK), using 63 × or 100 × oil immersion objectives (NA 1.32, zoom X). The fluorochromes were excited using an argon laser at 488 nm and a krypton laser at 568 nm. DAPI was excited with ultraviolet light using a 364 nm Argon laser. Detector slits were configured to minimize cross-talk between the channels. Differential interference contrast images were collected simultaneously with the fluorescence images, by the use of a transmitted light detector. Images were processed using FV10-ASW 1.4 Viewer and Adobe Photoshop 8.0 (Adobe Systems) software. Colocalization and deconvolution were performed using MetaMorph software (Molecular Devices, Silicon Valley, CA). Fluorescent images were observed with an inverted microscope (Carl Zeiss Axiovert 35M) equipped with epifluorescence and differential interference contrast (DIC) optics using a 100 × oil immersion objectives (Carl Zeiss) and were captured under regular fluorescence microscopy with a silicon-intensified target camera (SIT-C2400; Hamamatsu Phototonics, Bridgewater, NJ). The images were digitized directly into a Metamorph/Metafluor Image Processor (Universal Imaging Corporation, West Chester, PA).

Total internal reflection fluorescence microscopy (TIRFM)

ha–lrp trophozoites were grown in complete medium, collected, fixed using 1% glutaraldehyde, stained with FITC-labelled anti-HA mAb (diluted 1:200) followed by a second fixation with 1% glutaraldehyde/0.1 M glycine and attached to polylysine-treated coverslips. Alternatively, the *lrp–ha* and *lrp-FXNPXY–ha* trophozoites were permeabilized with 0.05% saponin in PBS after the first glutaraldehyde fixation and then processed as described. For positive and negative controls, anti-VSP9B10 mAb and the PV-marker LysoSensor were used, respectively, in cells fixed and treated with saponin before TIRFM. Trophozoites were observed using a 60 × 1.45 numerical aperture objective equipped for through-the-objective TIRF illumination using a 488 nm argon laser on a Nikon TE2000-U microscope with filter cubes optimized for fluorescein/GFP (Chroma Technology, Rockingham, VT). Images were captured with a cooled CCD ORCA II-ER (HAMAMATSU Photonics K.K., Shizuoka, Japan) camera and MetaMorph software (Molecular Devices, Silicon Valley, CA).

Bodipy-LDL

For colocalization of LDL/GlLRP, *lrp–ha* trophozoites were cultured for 2 days in a medium deficient in lipoprotein (Sigma), followed by a medium exchange for labelling buffer (50 mM glucose, 10 mM cysteine, 2 mM ascorbic acid in PBS, pH 7.1) containing 7.5 μg of Bodipy-labelled LDL. After 30 min at 37°C, the trophozoites were fixed, labelled with Alexa Fluor 555 anti-HA mAb and visualized by confocal microscopy. Twenty confocal sections of 0.4 μm were taken parallel to the coverslip (z sections).

Immunoprecipitation assay (IPP)

Wild-type, *lrp–ha*, *ha–lrp* and *lrp-FXNPXY–ha* trophozoites previously challenged with 10 μg ml^{-1} Bodipy-LDL (Invitrogen) or 100 μg ml^{-1} chylomicrons (Athens Research & Technology) were harvested and resuspended in 1 ml of cold lysis buffer (50 mM NaH_2PO_4, 300 mM NaCl, 1% Triton X-100) for 1 h at 4°C. The lysate was centrifuged at 10 000 *g* for 10 min at 4°C, and the supernatant mixed with anti-ApoB mAb and incubated overnight at 4°C. Protein A-agarose beads (50 μl; Qiagen, Valencia, CA) were added to each sample and incubated for 4 h at 4°C. Beads were pelleted at 700 *g* and washed four times with washing buffer (50 mM NaH_2PO_4, pH 8.0; 300 mM NaCl; 0.1% Triton X-100). Beads were resuspended in sample buffer and boiled for 10 min before immunoblot analysis using AP-labelled anti-HA mAb. Controls included testing of transgenic cell without addition of LDL or chylomicrons. Also, wild-type cells and a non-related mAb were used as controls of this assay. The IPP assay was repeated by growing the cells in growth medium containing 170 μg ml^{-1} PMSF before lipoprotein challenge and processed as described above. For the IPP shown in Fig. 10B, no inhibitors were used. In this assay the 2F5 mAb was utilized to immunoprecipitate μ2.

GlLRP downregulation

From 1 to 2244 of the *gllrp* ORF was amplified using the f3 (CATTGATATCATGCATGCAGTGATCTACGGATTGCTTGTC) and r3 (CATTCCATGGTTAGTGGTGGGAGGAATAGAGCA) primers, restricted with EcoRV and NcoI enzymes and ligated to **p**TubHAc-pac vector in the opposite direction, resulting in the antisense vector that was used for inhibition of GlLRP expression. The **p**LRP-AS vector was used to stably transfect the *Giardia* clone WB1267, producing *lrp:as* cells deficient in GlLRP. Antisense production as well as *gllrp* depletion was confirmed by RT-PCR before performing the uptake experiments.

Semi-quantitative RT-PCR

The total RNA from wild-type and *lrp:as* cells was isolated using Trizol reagent (Invitrogen), and a second purification was performed using the SV Total RNA Isolation System (Promega). Semi-quantitative RT-PCR was performed as previously described (Rivero *et al.*, 2010). For detection of

endogenous *gllrp* mRNA, the f4 (CGTGCGCATCACCTTT-TACGATAGTAT) and r1 primers corresponding to the 3′ 2451–3213 nt were used. To detect the *gllrp* antisense, the r3 primer was added during the reverse transcription step, followed by the addition of the f3 primer for PCR amplification. These assays were performed four times in duplicates.

Uptake experiments

The Bodipy-LDL uptake assays were performed as reported (Rivero *et al*., 2010). Briefly, wild-type, *lrp:as*, *ha–lrp* and *lrp-FXNPXY–ha* trophozoites were cultured for 2 days in medium deficient in lipoprotein and the uptake was performed by exchanging the medium for labelling buffer containing 7.5 μg of Bodipy-labelled LDL. After different time periods at 37°C, the trophozoites were washed and visualized by fluorescence microscopy. All images were acquired and processed identically. Fluorescence images were measured by Metamorph software version 7.0. All the images were equally processed; the threshold value was determined and exclusive in each image. Controls for this experiment included the addition of 2 mg ml^{-1} FITC-dextran (Sigma) or 10 μM LysoTracker Red DND-99 (Molecular Probes-Invitrogen) to the tested trophozoites for 30 min.

Growth curve

Tubes containing 7 ml of growth medium were inoculated with 10^4 trophozoites from wild-type (*wt*) or GlLRP antisense transgenic (*lrp:as*) trophozoites logarithmic phase cultures. Every 6 h, the medium was decanted and the tubes were chilled on ice for 20 min to detach adherent living trophozoites. The number of viable cells was determined by counting on a haemocytometer. Cells expressing the empty antisense vector or a non-related GSP:antisense vector (Touz *et al*., 2002b) were used as control.

Yeast two-hybrid assay

The MATCHMAKER Two-Hybrid System was used following the manufacturer's recommended protocol (Clontech, Palo Alto, CA). The two-hybrid **p**GADT7-Rec(LEU2) vector (GAL4 transcription activation domain; AD) containing the sequences for gl*lrp* or *lrp-FXNPXY* [lacking the FXNPXY-like motif sequence (3′-AATAGCCCCACATAT)] was used as bait, while *μ2* gene was inserted into the **p**GBKT7(TRP1) vector (GAL4 DNA-binding domain; BD), yielding the **p**LRP-AD, **p**LRP-FXNPXY-AD and **p**μ2-BD vectors respectively. The AH109 transformants were cultured at 30°C for 4–5 days on plates with minimal medium lacking leucine and tryptophan (–L/–T) to test for positive transformation, or in the absence of leucine, tryptophan and histidine (TDO, triple dropout medium) to study specific protein interactions as previously described (Touz *et al*., 2004). Controls included the **p**β2-AD/**p**μ2-BD interaction (positive control) and the empty **p**GADT7/**p**μ2-BD vector (negative control).

Statistics

Descriptive statistics included the calculation of the means and standard deviations of the control and experimental groups. A comparison of the means was performed using the Independent-Samples Student's *t*-test from the SPSS Statistic program. A $P \leq 0.05$ was considered significant.

Acknowledgements

We thank Dr Mariano Bisbal and Ignacio Jausoro for TIRF microscopy assistance. We also thank members of our laboratory for helpful discussions. The project was supported by Grant No. R01TW00724 from the Fogarty International Center. The content is solely the responsibility of the authors and does not necessarily represent the official views of the Fogarty International Center or the National Institutes of Health. This research was also supported in part by the Academy of Science for the Developing World (TWAS), Agencia Nacional para la Promoción de la Ciencia y Tecnología (FONCyT) PICT2004-PICT2007, and the National Council for Sciences and Technology (CONICET) PIP2005-6563.

References

Adam, R.D. (2001) Biology of *Giardia lamblia*. *Clin Microbiol Rev* **14:** 447–475.

Ashworth, J.L., Kelly, V., Rock, M.J., Shuttleworth, C.A., and Kielty, C.M. (1999a) Regulation of fibrillin carboxy-terminal furin processing by N-glycosylation, and association of amino- and carboxy-terminal sequences. *J Cell Sci* **112** (Part 22)**:** 4163–4171.

Ashworth, J.L., Murphy, G., Rock, M.J., Sherratt, M.J., Shapiro, S.D., Shuttleworth, C.A., and Kielty, C.M. (1999b) Fibrillin degradation by matrix metalloproteinases: implications for connective tissue remodelling. *Biochem J* **340** (Part 1)**:** 171–181.

Axelrod, D. (1989) Total internal reflection fluorescence microscopy. *Methods Cell Biol* **30:** 245–270.

Axelrod, D. (2003) Total internal reflection fluorescence microscopy in cell biology. *Methods Enzymol* **361:** 1–33.

Boll, W., Rapoport, I., Brunner, C., Modis, Y., Prehn, S., and Kirchhausen, T. (2002) The mu2 subunit of the clathrin adaptor AP-2 binds to FDNPVY and YppO sorting signals at distinct sites. *Traffic* **3:** 590–600.

Delcamp, T.J., Dales, C., Ralenkotter, L., Cole, P.S., and Hadley, R.W. (1998) Intramitochondrial [Ca2+] and membrane potential in ventricular myocytes exposed to anoxia-reoxygenation. *Am J Physiol* **275:** H484–H494.

Duckert, P., Brunak, S., and Blom, N. (2004) Prediction of proprotein convertase cleavage sites. *Protein Eng Des Sel* **17:** 107–112.

Elmendorf, H.G., Singer, S.M., Pierce, J., Cowan, J., and Nash, T.E. (2001) Initiator and upstream elements in the alpha2-tubulin promoter of *Giardia lamblia*. *Mol Biochem Parasitol* **113:** 157–169.

Gallego, E., Alvarado, M., and Wasserman, M. (2007) Identification and expression of the protein ubiquitination system in *Giardia intestinalis*. *Parasitol Res* **101:** 1–7.

Goretzki, L., and Mueller, B.M. (1998) Low-density-lipoprotein-receptor-related protein (LRP) interacts with a GTP-binding protein. *Biochem J* **336** (Part 2)**:** 381–386.

Harris-White, M.E., and Frautschy, S.A. (2005) Low density lipoprotein receptor-related proteins (LRPs), Alzheimer's

and cognition. *Curr Drug Targets CNS Neurol Disord* **4:** 469–480.

Herz, J., and Strickland, D.K. (2001) LRP: a multifunctional scavenger and signaling receptor. *J Clin Invest* **108:** 779–784.

Herz, J., Hamann, U., Rogne, S., Myklebost, O., Gausepohl, H., and Stanley, K.K. (1988) Surface location and high affinity for calcium of a 500-kd liver membrane protein closely related to the LDL-receptor suggest a physiological role as lipoprotein receptor. *EMBO J* **7:** 4119–4127.

Herz, J., Kowal, R.C., Goldstein, J.L., and Brown, M.S. (1990) Proteolytic processing of the 600 kd low density lipoprotein receptor-related protein (LRP) occurs in a *trans*-Golgi compartment. *EMBO J* **9:** 1769–1776.

Jeon, H., Meng, W., Takagi, J., Eck, M.J., Springer, T.A., and Blacklow, S.C. (2001) Implications for familial hypercholesterolemia from the structure of the LDL receptor YWTD-EGF domain pair. *Nat Struct Biol* **8:** 499–504.

Jones, C., Hammer, R.E., Li, W.P., Cohen, J.C., Hobbs, H.H., and Herz, J. (2003) Normal sorting but defective endocytosis of the low density lipoprotein receptor in mice with autosomal recessive hypercholesterolemia. *J Biol Chem* **278:** 29024–29030.

Kaul, D., and Kaur, M. (2001) Receptor-Ck regulates membrane-bound 125 kDa protein having affinity for genomic sterol regulatory sequence. *Mol Cell Biochem* **216:** 141–143.

Keister, D.B. (1983) Axenic culture of *Giardia lamblia* in TYI-S-33 medium supplemented with bile. *Trans R Soc Trop Med Hyg* **77:** 487–488.

Krieger, M., and Herz, J. (1994) Structures and functions of multiligand lipoprotein receptors: macrophage scavenger receptors and LDL receptor-related protein (LRP). *Annu Rev Biochem* **63:** 601–637.

Kulakova, L., Singer, S.M., Conrad, J., and Nash, T.E. (2006) Epigenetic mechanisms are involved in the control of *Giardia lamblia* antigenic variation. *Mol Microbiol* **61:** 1533–1542.

Li, Y., Cam, J., and Bu, G. (2001) Low-density lipoprotein receptor family: endocytosis and signal transduction. *Mol Neurobiol* **23:** 53–67.

Liu, C.X., Ranganathan, S., Robinson, S., and Strickland, D.K. (2007) Gamma-secretase-mediated release of the low density lipoprotein receptor-related protein 1B intracellular domain suppresses anchorage-independent growth of neuroglioma cells. *J Biol Chem* **282:** 7504–7511.

Logeat, F., Bessia, C., Brou, C., LeBail, O., Jarriault, S., Seidah, N.G., and Israel, A. (1998) The Notch1 receptor is cleaved constitutively by a furin-like convertase. *Proc Natl Acad Sci USA* **95:** 8108–8112.

Lujan, H.D., Mowatt, M.R., Helman, L.J., and Nash, T.E. (1994) Insulin-like growth factors stimulate growth and L-cysteine uptake by the intestinal parasite *Giardia lamblia*. *J Biol Chem* **269:** 13069–13072.

Lujan, H.D., Mowatt, M.R., and Nash, T.E. (1996a) Lipid requirements and lipid uptake by *Giardia lamblia* trophozoites in culture. *J Eukaryot Microbiol* **43:** 237–242.

Lujan, H.D., Mowatt, M.R., Conrad, J.T., and Nash, T.E. (1996b) Increased expression of the molecular chaperone BiP/GRP78 during the differentiation of a primitive eukaryote. *Biol Cell* **86:** 11–18.

Misra, U.K., Gawdi, G., Gonzalez-Gronow, M., and Pizzo, S.V. (1999) Coordinate regulation of the alpha(2)-macroglobulin signaling receptor and the low density lipoprotein receptor-related protein/alpha(2)-macroglobulin receptor by insulin. *J Biol Chem* **274:** 25785–25791.

Nash, T.E., Aggarwal, A., Adam, R.D., Conrad, J.T., and Merritt, J.W., Jr. (1988) Antigenic variation in *Giardia lamblia*. *J Immunol* **141:** 636–641.

Nash, T.E., Lujan, H.T., Mowatt, M.R., and Conrad, J.T. (2001) Variant-specific surface protein switching in *Giardia lamblia*. *Infect Immun* **69:** 1922–1923.

Newman, Z.L., Leppla, S.H., and Moayeri, M. (2009) CA-074Me protection against anthrax lethal toxin. *Infect Immun* **77:** 4327–4336.

Obermoeller-McCormick, L.M., Li, Y., Osaka, H., FitzGerald, D.J., Schwartz, A.L., and Bu, G. (2001) Dissection of receptor folding and ligand-binding property with functional minireceptors of LDL receptor-related protein. *J Cell Sci* **114:** 899–908.

Rebeck, G.W., LaDu, M.J., Estus, S., Bu, G., and Weeber, E.J. (2006) The generation and function of soluble apoE receptors in the CNS. *Mol Neurodegener* **1:** 15.

Reekmans, S.M., Pflanzner, T., Gordts, P.L., Isbert, S., Zimmermann, P., Annaert, W., *et al*. (2010) Inactivation of the proximal NPXY motif impairs early steps in LRP1 biosynthesis. *Cell Mol Life Sci* **67:** 135–145.

Rivero, M.R., Vranych, C.V., Bisbal, M., Maletto, B.A., Ropolo, A.S., and Touz, M.C. (2010) Adaptor protein 2 regulates receptor-mediated endocytosis and cyst formation in *Giardia lamblia*. *Biochem J* **428:** 33–45.

Rudenko, G., Henry, L., Henderson, K., Ichtchenko, K., Brown, M.S., Goldstein, J.L., and Deisenhofer, J. (2002) Structure of the LDL receptor extracellular domain at endosomal pH. *Science* **298:** 2353–2358.

Sali, A., Potterton, L., Yuan, F., van Vlijmen, H., and Karplus, M. (1995) Evaluation of comparative protein modeling by MODELLER. *Proteins* **23:** 318–326.

Shen, M.Y., and Sali, A. (2006) Statistical potential for assessment and prediction of protein structures. *Protein Sci* **15:** 2507–2524.

Singer, S.M., Yee, J., and Nash, T.E. (1998) Episomal and integrated maintenance of foreign DNA in *Giardia lamblia*. *Mol Biochem Parasitol* **92:** 59–69.

Steiner, D.F. (1998) The proprotein convertases. *Curr Opin Chem Biol* **2:** 31–39.

Takeda, T., Yamazaki, H., and Farquhar, M.G. (2003) Identification of an apical sorting determinant in the cytoplasmic tail of megalin. *Am J Physiol Cell Physiol* **284:** C1105–C1113.

Touz, M.C., Nores, M.J., Slavin, I., Carmona, C., Conrad, J.T., Mowatt, M.R., *et al*. (2002a) The activity of a developmentally regulated cysteine proteinase is required for cyst wall formation in the primitive eukaryote *Giardia lamblia*. *J Biol Chem* **277:** 8474–8481.

Touz, M.C., Gottig, N., Nash, T.E., and Lujan, H.D. (2002b) Identification and characterization of a novel secretory granule calcium-binding protein from the early branching eukaryote *Giardia lamblia*. *J Biol Chem* **277:** 50557–50563.

Touz, M.C., Lujan, H.D., Hayes, S.F., and Nash, T.E. (2003) Sorting of encystation-specific cysteine protease to

lysosome-like peripheral vacuoles in *Giardia lamblia* requires a conserved tyrosine-based motif. *J Biol Chem* **278:** 6420–6426.

Touz, M.C., Kulakova, L., and Nash, T.E. (2004) Adaptor protein complex 1 mediates the transport of lysosomal proteins from a Golgi-like organelle to peripheral vacuoles in the primitive eukaryote *Giardia lamblia*. *Mol Biol Cell* **15:** 3053–3060.

Touz, M.C., Conrad, J.T., and Nash, T.E. (2005) A novel palmitoyl acyl transferase controls surface protein palmitoylation and cytotoxicity in *Giardia lamblia*. *Mol Microbiol* **58:** 999–1011.

Trommsdorff, M., Borg, J.P., Margolis, B., and Herz, J. (1998) Interaction of cytosolic adaptor proteins with neuronal apolipoprotein E receptors and the amyloid precursor protein. *J Biol Chem* **273:** 33556–33560.

Trommsdorff, M., Gotthardt, M., Hiesberger, T., Shelton, J., Stockinger, W., Nimpf, J., *et al*. (1999) Reeler/Disabled-like disruption of neuronal migration in knockout mice lacking the VLDL receptor and ApoE receptor 2. *Cell* **97:** 689–701.

Tung, C.W., and Ho, S.Y. (2008) Computational identification of ubiquitylation sites from protein sequences. *BMC Bioinformatics* **9:** 310.

Veniant, M.M., Zlot, C.H., Walzem, R.L., Pierotti, V., Driscoll, R., Dichek, D., *et al*. (1998) Lipoprotein clearance mechanisms in LDL receptor-deficient 'Apo-B48-only' and 'Apo-B100-only' mice. *J Clin Invest* **102:** 1559–1568.

Waldron, E., Heilig, C., Schweitzer, A., Nadella, N., Jaeger, S., Martin, A.M., *et al*. (2008) LRP1 modulates APP trafficking along early compartments of the secretory pathway. *Neurobiol Dis* **31:** 188–197.

Ward, D.M., Ajioka, R., and Kaplan, J. (1989) Cohort movement of different ligands and receptors in the intracellular endocytic pathway of alveolar macrophages. *J Biol Chem* **264:** 8164–8170.

Wassler, M., Jonasson, I., Persson, R., and Fries, E. (1987) Differential permeabilization of membranes by saponin treatment of isolated rat hepatocytes. Release of secretory proteins. *Biochem J* **247:** 407–415.

Willnow, T.E., and Herz, J. (1995) Animal models for disorders of hepatic lipoprotein metabolism. *J Mol Med* **73:** 213–220.

Willnow, T.E., Armstrong, S.A., Hammer, R.E., and Herz, J. (1995) Functional expression of low density lipoprotein receptor-related protein is controlled by receptor-associated protein *in vivo*. *Proc Natl Acad Sci USA* **92:** 4537–4541.

Willnow, T.E., Nykjaer, A., and Herz, J. (1999) Lipoprotein receptors: new roles for ancient proteins. *Nat Cell Biol* **1:** E157–E162.

Yee, J., and Nash, T.E. (1995) Transient transfection and expression of firefly luciferase in *Giardia lamblia*. *Proc Natl Acad Sci USA* **92:** 5615–5619.

Yu, K.C., Chen, W., and Cooper, A.D. (2001) LDL receptor-related protein mediates cell-surface clustering and hepatic sequestration of chylomicron remnants in LDLR-deficient mice. *J Clin Invest* **107:** 1387–1394.

Zemskov, E.A., Mikhailenko, I., Strickland, D.K., and Belkin, A.M. (2007) Cell-surface transglutaminase undergoes internalization and lysosomal degradation: an essential role for LRP1. *J Cell Sci* **120:** 3188–3199.

Supporting information

Additional supporting information may be found in the online version of this article.

Please note: Wiley-Blackwell are not responsible for the content or functionality of any supporting materials supplied by the authors. Any queries (other than missing material) should be directed to the corresponding author for the article.